Proceedings of the IASS Annual Symposium 2025
"The living past as a source of innovation"
October 27 – 31, 2025, México City, México
Juan Gerardo Oliva, Juan Ignacio del Cueto, Elisa Drago Quaglia (eds.)

Numerical Modeling and Structural Analysis of Compression-Dominant Multi-Layer Funicular Glass Bridges

Fahimeh YAVARTANOO^a, Damon BOLHASSANI*, Masoud AKBARZADEH^b, Yao LU^b, Joseph R. YOST^c, Jorge H. CHACON^c, and Philipp A. CHHADEH^d

*, a ABC Lab, Spitzer School of Architecture, The City College of New York (CCNY), New York, USA mbolhassani@ccny.cuny.edu

Polyhedral Structures Laboratory, University of Pennsylvania
 Villanova University
 d Technische Universit at Darmstadt

Abstract

This study presents a numerical modeling framework for analyzing the structural behavior of a compression-dominant, multi-layer, sheet-based funicular glass bridge. A finite element (FE) model was first developed and verified using a 3.3-meter glass bridge prototype, which was subsequently calibrated against experimental results from tests conducted at Villanova University. Upon successful validation, the numerical methodology was extended to simulate a 10-meter bridge prototype, assessing its structural response under applied loading conditions. The 3.3-meter bridge model consists of hollow glass units (HGUs), with float glass plates for the top and bottom decks and acrylic side plates for lateral support. In the physical experiment, VBH structural tape was used for deck-side plate connections, while Surlyn thermoplastic and acrylic locking bars served as joint interfaces. However, to simplify the numerical model, a semi-micro modeling approach was adopted, representing the bridge as fully jointed acrylic side plates with glass decks placed on top and bottom surfaces. The finite element (FE) model was constructed in ABAQUS, employing solid elements for the side plates and shell elements for the glass decks. Cohesive and frictional contact interactions were defined using a small sliding formulation and surface-to-surface discretization. The model incorporated pinned boundary conditions at both ends, replacing the steel abutments used in the physical prototype. A displacement-control approach was employed for loading, replicating the experimental test conditions. The findings indicated that the numerical model effectively captured the structural behavior of the glass bridge, demonstrating good agreement with experimental observations. The stress distribution analysis suggests an efficient load transfer mechanism, with tensile stresses concentrated in critical regions such as the mid-span and near the supports. The validated FEM approach provides a reliable and computationally efficient methodology for assessing the performance of segmental glass bridge structures, offering valuable insights into stress distribution, deformation behavior, and load-bearing capacity. Moreover, this study highlights the potential of numerical modeling to complement experimental testing, reducing the need for extensive physical trials and paving the way for further research into compression-based glass structures and innovative bridge designs.

Keywords: Funicular glass bridge, FEM, Compression-dominant structure, Segmental glass construction, Structural performance evaluation, Numerical validation, Calibration, ABAQUS.

1. Introduction

The use of glass as a structural material has evolved significantly, moving beyond its traditional role in architectural applications to serve in primary load-bearing functions, particularly in pedestrian bridges and transparent infrastructure. Glass offers a unique blend of mechanical performance and aesthetic appeal, characterized by high compressive strength, dimensional stability, and optical clarity. These properties make it increasingly attractive for use not just as a façade or enclosure, but as an active structural element. In particular, the application of glass sheets in multi-layer, sheet-based structures has gained momentum, as designers and engineers explore its viability for in-plane load-bearing applications. Rather than serving merely architectural purposes, glass is now being strategically integrated into systems that exploit compression-dominant force paths, allowing it to function effectively as an axially loaded compression member. This shift reflects a growing recognition of glass's potential to contribute meaningfully to the structural integrity of lightweight, modular, and transparent systems [1-2]. However, its brittle fracture behavior, low tensile strength, and sensitivity to edge defects present significant challenges for structural applications, particularly when subjected to tension or bending [3-4].

These limitations necessitate innovative approaches to both geometry and construction techniques, emphasizing compression-dominant design and precise assembly methods. Recent developments in modular construction and polyhedral graphic statics (PGS) have enabled a new generation of glass structures that address these challenges. Notably, Three-Dimensional Graphic Statics (TDGS) has been introduced to form structural systems where internal forces remain primarily compressive [5-7]. These tools allow the creation of spatial geometries that are inherently stable and tailored to exploit the compressive strength of flat sheet materials, especially glass. This design paradigm has resulted in several modular prototypes, including the recently developed *Tortuca* bridge, a 3.3-meter span shell-type structure assembled entirely from Hollow Glass Units (HGUs) [8].

The *Tortuca* prototype consists of 13 interlocking HGUs, each composed of float glass deck plates and acrylic side plates, joined by 3MTM VHB tape, Surlyn interface sheets, and mechanical locking bars. The structural behavior of this system under service loading was experimentally evaluated, confirming the feasibility of compression-based force flow, segmental interlocking, and adhesive interface systems for modular glass bridge construction. Measured deflections remained within L/610, well below the AASHTO serviceability limits, while strain readings confirmed the presence of compression at the bottom deck and tensile behavior at the top, particularly in midspan segments. This experiment provided critical insights into the physical performance of modular glass bridges, while also highlighting the need for advanced numerical modeling to predict behavior in larger, untested spans. In parallel, Bolhassani et al. [9] developed a comprehensive numerical modeling framework for a similar 3.3-meter modular glass bridge using micro-scale finite element analysis. Their study emphasized the importance of modeling cohesive and frictional interactions, geometric nonlinearity, and the assembly sequence, all of which significantly affect the system's behavior. The model showed good agreement with experimental measurements, with maximum displacements and stress distributions aligning closely with test data.

While these initial studies laid a strong foundation, the literature on numerical modeling and calibration of modular glass bridges remains scarce. The need for rigorous simulation, rooted in test data and calibrated using physical prototypes, is critical to ensure safety, performance, and regulatory compliance in such pioneering structural applications. This study aims to address this gap by presenting a comprehensive numerical modeling methodology, calibrated against experimental data from the 3.3-meter *Tortuca* bridge, and extended to simulate the performance of the 10-meter bridge design. The numerical model uses a simplified micro-modeling approach, balancing detail and computational efficiency. Key interactions, frictional and cohesive, are selectively applied across interfaces, and material properties are defined based on experimental data. The model accounts for contact behavior, geometry-induced nonlinearities, and modular segmentation. Validation is achieved by comparing

Proceedings of the IASS Annual Symposium 2025 The living past as a source of innovation

numerical predictions with measured displacements under service loading, providing confidence in the reliability of the FE model.

The contributions of this paper are threefold: It introduces a refined FEM approach for modeling large-span modular glass bridges; it establishes a direct calibration methodology grounded in physical testing; and it applies this method to the 10-meter span design, offering predictive insights into stress distribution, deformation behavior, and structural safety. By integrating experimental and numerical studies, this work seeks to advance the engineering understanding of modular all-glass bridge systems and lay the groundwork for their broader adoption in transparent infrastructure design.

2. Numerical modeling approach

Numerical simulations were conducted using ABAQUS [10] to evaluate the structural behavior of modular glass pedestrian bridges under applied loading. The models were developed to reflect realistic structural performance by incorporating key factors such as material properties, contact interactions, boundary conditions, and meshing schemes. Two configurations were analyzed: a 3.3-meter prototype, used for model calibration against experimental data, and a 10-meter span, evaluated using the validated model. By maintaining consistent modeling parameters across both cases, a direct performance comparison was enabled.

2.1. Material

The pedestrian glass bridge is composed of glass panels, acrylic side plates, Surlyn sheets, and $3M^{TM}$ VHB tape, each contributing to the structure's performance and assembly. The 9.5 mm float glass plates, used for the top and bottom surfaces of each HGU. The 21 mm acrylic side plates enhance lateral confinement and segmental stability and are also shaped to accommodate connection features. Surlyn sheets are placed between units to prevent direct acrylic-to-acrylic contact, improving load transfer and post-fracture behavior. VHB tape provides transparent, high-strength adhesive bonding between glass and acrylic, enabling modular construction without mechanical fasteners. Locking bars reinforce the junctions between units, supporting interlocking behavior and minimizing stress concentrations at edges. In the FE model, only glass and acrylic are explicitly assigned material properties, both modeled as linear elastic. Glass is modeled with E = 65,000 MPa, $\rho = 2500$ kg/m³, v = 0.22, and acrylic with E = 1000 MPa, $\rho = 1180$ kg/m³, v = 0.4. The effects of Surlyn, VHB, and locking strips are captured through interaction properties, such as cohesive and frictional contacts, rather than through separate material definitions, simplifying the model while preserving essential mechanical behavior.

2.2. Interaction

The structural performance of the modular glass bridge depends on the complex interplay between various components, including glass deck plates, acrylic side plates, 3MTM VHB structural tape, locking bars, and Surlyn interface sheets placed between segments. When modeled in full detail, this system includes over 124 interlocking segments for 10-m prototype, each contributing to a large number of nonlinear interactions and contact interfaces (more than 2000 interactions). Accurately capturing every material layer and joint would result in an exceedingly large and computationally intensive model. To address this, three modeling strategies were considered: micro-modeling, macro-modeling, and a simplified micro-modeling approach. The micro-modeling strategy involves explicitly representing all individual materials and interfaces, glass, acrylic, adhesives, and interlayers, along with their respective geometries and behaviors, including frictional slip and cohesive bonding. While this method provides high resolution and realism, it becomes computationally unmanageable for full-scale systems due to the volume of contact definitions and convergence challenges. Moreover, many internal interactions have minimal effect on global response and therefore do not justify the computational burden. In contrast, the macro-modeling approach simplifies the entire bridge as a continuous monolithic entity with homogenized material properties. Although this drastically reduces modeling complexity and runtime,

it fails to capture the segmented nature of the bridge and lacks the ability to reflect joint flexibility, interlocking behavior, or local failure mechanisms, key characteristics of modular glass structures. Due to these limitations, this approach was deemed unsuitable for the present study. To balance detail and efficiency, this study adopts a simplified micro-modeling approach [10] (Figure 1). The bridge is still treated as a segmented system, preserving the geometry and interaction between modular units, but without modeling each interlayer or adhesive surface in full detail. The glass and acrylic plates in each segment are treated as unified components, with tie constraints applied between them to ensure complete transfer of displacement and rotation, effectively simulating the bonded composite behavior of HGUs. This reduced the model size while maintaining accurate simulation of the bridge's primary load path and deformation response.

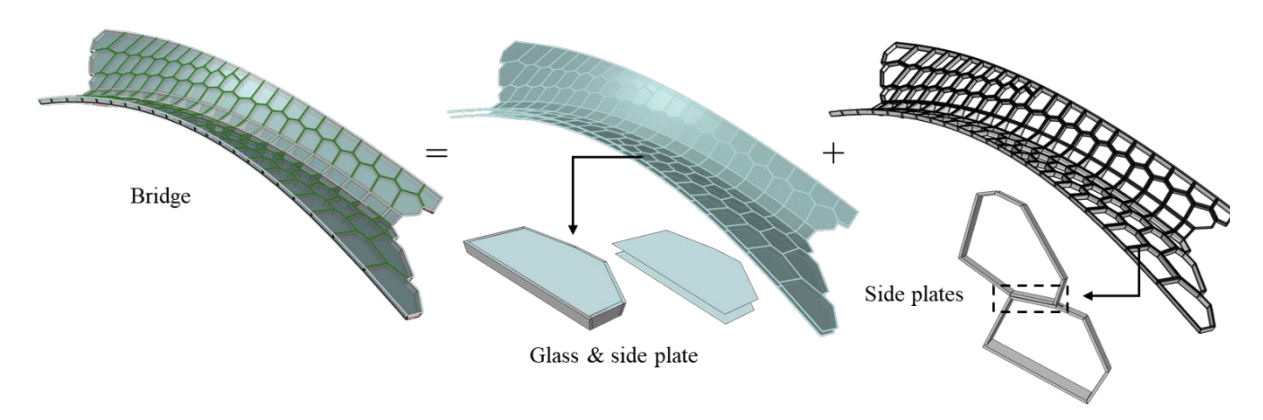


Figure 1. Simplified micro-modeling approach

Despite the simplification, modeling the interactions between segments remained challenging, particularly in defining the appropriate contact behavior in the absence of locking bars. A hybrid contact strategy was implemented to realistically simulate the mechanical behavior between adjacent segments. At joints equipped with locking bars, cohesive contact definitions were assigned to capture the interlocking effect. These were modeled using a traction-separation law with uncoupled stiffness in the normal and shear directions, allowing limited relative displacement while resisting pull-out and sliding, effectively simulating the mechanical engagement provided by the physical locks and Surlyn interfaces. Conversely, at joints without locking bars, frictional contact was applied using a penalty formulation, hard contact in the normal direction, and the option to allow separation under tension. This selective assignment of contact properties based on physical connection type reflects the real assembly logic of the bridge and ensures the accurate transfer of forces across segments. It also improves numerical stability and preserves the essential interaction behavior needed for reliable structural response predictions.

2.3. **Mesh**

The finite element mesh was designed to balance computational efficiency with the need to accurately capture the complex mechanical behavior of the structure. Reflecting the hybrid nature of the simplified micro-modeling approach, two element types were used: S4R shell elements for the glass deck plates and C3D8R solid brick elements for the acrylic side plates. The top and bottom glass plates of each HGU were modeled with four-node, reduced integration shell elements (S4R) to simulate bending and membrane action effectively. A uniform mesh size of 25 mm was applied, based on preliminary sensitivity studies, ensuring sufficient resolution without excessive computational cost. Reduced integration minimized shear locking and improved convergence. The acrylic side plates were meshed

using 8-node solid elements with reduced integration (C3D8R) to better resolve 3D stress states, particularly around contact and joint regions. The same 25 mm mesh size was maintained to ensure compatibility across tie and contact interfaces. The resulting structured mesh supported stable interaction definitions between glass and acrylic components, as illustrated in Figure 2a and b.

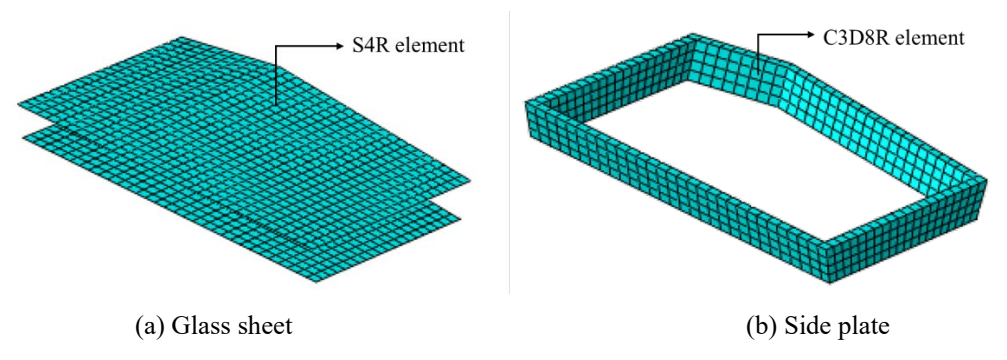


Figure 2. Element type

3. Calibration and validation (3.3-m bridge)

The numerical model was calibrated using data from a full-scale test of a 3.3-meter modular glass bridge prototype, Tortuca, developed by Yost et al. [8]. The structure consists of 13 HGUs formed from float glass deck plates and acrylic side plates, bonded with 3MTM VHB tape, and separated at joints using Surlyn interlayers to prevent brittle contact. The geometry of bridge, derived through 3DGS, was designed by Lu et al. [2] to promote in-plane compression and minimize tensile stress in the glass. The prototype was supported on steel abutments, with diagonal steel ties in an X-configuration to simulate shell thrust resistance, conditions replicated in the FE model. A displacement-controlled vertical load of 7.1 kN was applied using a hydraulic actuator, distributed across the north-south joints between HGUs 2-6 and 6-7 (Figure 3). Notably, one joint lacked a locking bar, introducing contrast in local stiffness, which was reflected in the simulation via adjusted contact properties. The loading sequence included two phases: (1) service loading and unloading (0.71-7.1 kN), and (2) a 14.7-hour recovery period to observe viscoelastic effects. Instrumentation involved 13 vertical displacement sensors and 10 strain rosettes mounted on selected HGUs. The maximum midspan deflection reached ~5.5 mm at HGU-6, with residual deformation of ~0.97 mm, half of which recovered within 3 hours. Measured strains (~105 με in tension, ~110 με in compression) yielded stress values of ~7.35 MPa and ~7.70 MPa, validating the model's assumptions under service conditions. These results informed the calibration of contact behaviors, material stiffness, and time-dependent responses in the simulation.

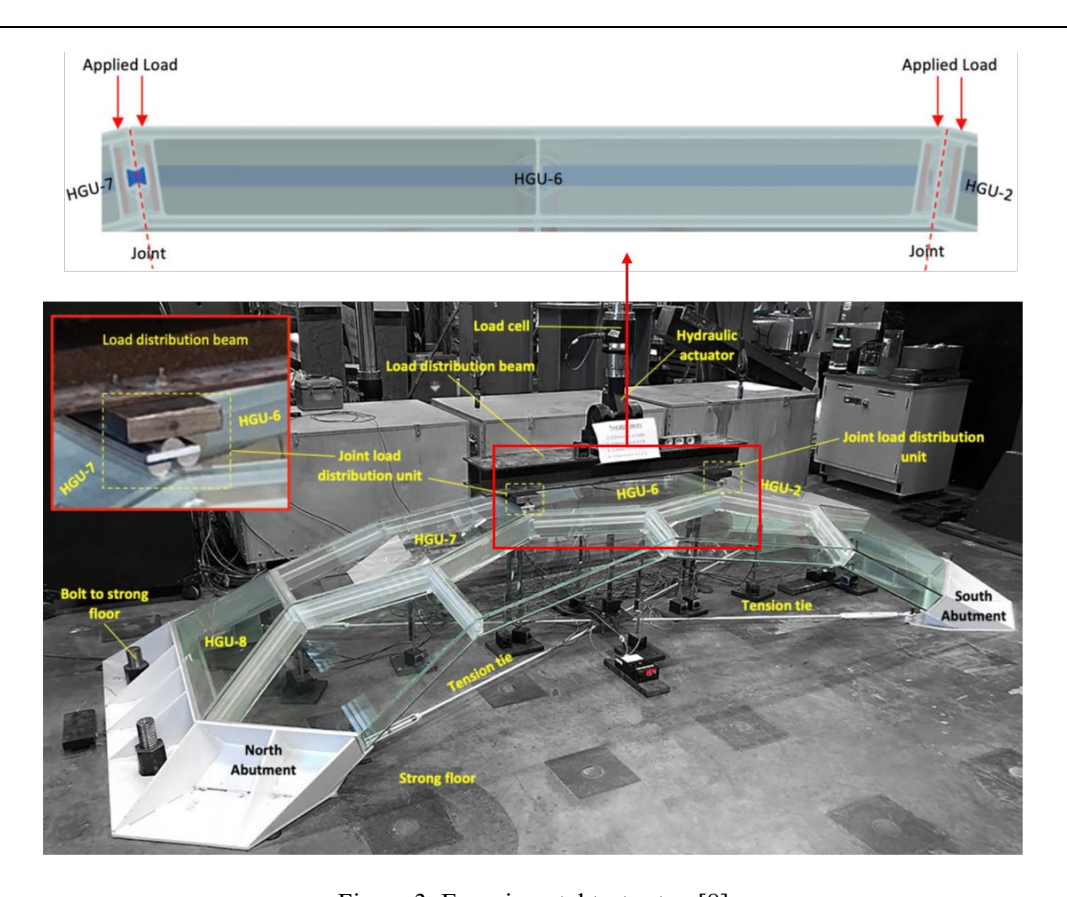


Figure 3. Experimental test setup [8]

The finite element model of the 3.3-meter modular glass bridge was configured to replicate the conditions observed during the physical experimental test. The boundary conditions were designed to simulate realistic support and loading configurations, enabling accurate model calibration and validation. As shown in Figure 4, both ends of the bridge were modeled with fully fixed supports, where all translational (U1, U2, U3) and rotational (UR1, UR2, UR3) degrees of freedom were restrained. This configuration corresponds to the bridge's anchorage to rigid steel abutments bolted to the laboratory strong floor, effectively eliminating any rigid body motion and rotation at the supports. Although the physical system includes tension ties between abutments to resist outward thrust, the full constraint applied in the model simplifies this effect by directly enforcing global stability. This setup ensures accurate load transfer into the supports and provides a consistent baseline for validating structural deformation and stress responses under applied loads.

A gravity load was applied uniformly across the model to simulate self-weight, taking into account the material densities of glass and acrylic as defined in the material module. To simulate the experimental loading phase, a displacement-controlled vertical load was applied at the interface joints between HGU-6 and HGU-2 and between HGU-6 and HGU-7. The magnitude of the imposed displacement was 6 mm, corresponding to the actuator displacement used in the physical test. This load was applied symmetrically to match the experimental loading setup, which used distribution beams to ensure uniform force application across the bridge width.

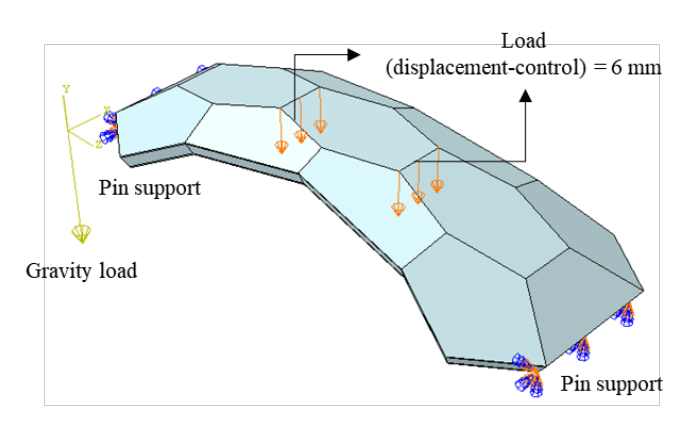


Figure 4. Load and boundary conditions of 3.3-m glass bridge prototype

Figure 5 presents the comparison between the experimental and numerical responses of the 3.3-meter modular glass bridge under a vertical load of 7.1 kN. The load-displacement curve shows close agreement between the finite element model (FEM) and experimental (EXP) results in the elastic range. However, as the load increases, a divergence is observed: the FEM predicts a stiffer response, with a maximum midspan displacement of 3.69 mm, while the experiment recorded a larger displacement of 4.3 mm (Figure 5a). This deviation is attributed to several factors, including idealized material behavior (linear elasticity), simplified interface modeling, and the absence of minor imperfections or microcracking in the numerical model. Figure 5b presents the vertical displacement profile along the HGUs of the 3.3-meter modular glass bridge, comparing results from the experiment (black line) and the finite element model (red line). Both curves exhibit a symmetrical deflection pattern, characteristic of shelltype structures under uniform vertical loading, with maximum displacement occurring at HGU-6, near the midspan. While the FE model slightly underestimates displacement across the span, the overall shape and trend closely mirror the experimental data, validating the ability of the simplified micro-modeling approach to capture the global deformation behavior of the bridge. The alignment in deflection mode shape affirms that the model accurately represents the structural stiffness and boundary conditions, despite minor differences in magnitude likely due to idealized material behavior and simplified joint representations.

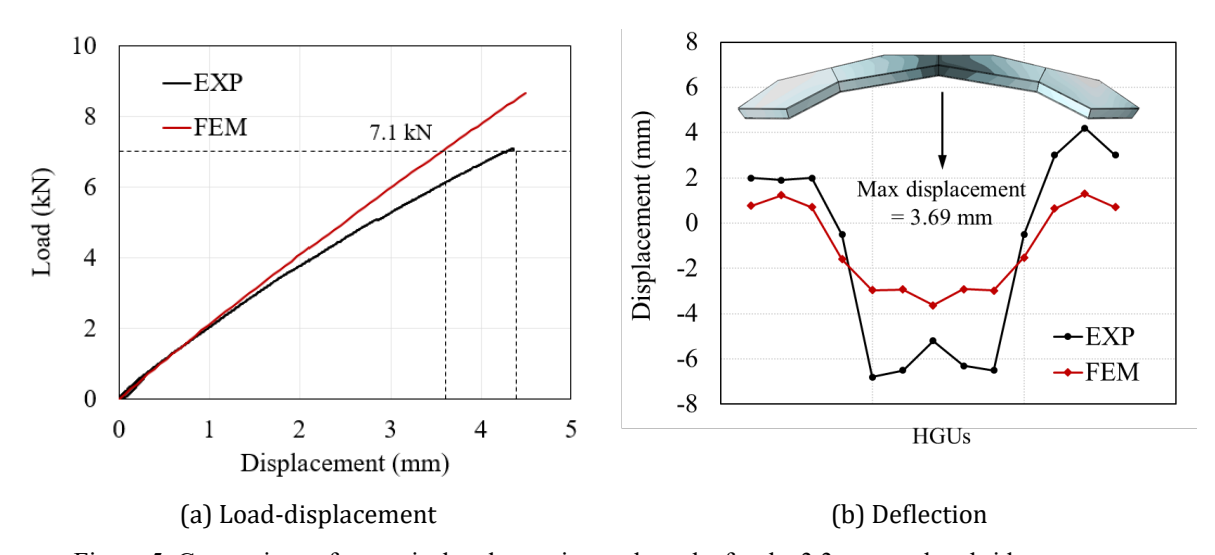


Figure 5. Comparison of numerical and experimental results for the 3.3-meter glass bridge prototype

Figure 6 illustrates the distribution of maximum and minimum principal stresses in the 3.3-meter modular glass bridge model under a displacement of 4.5 mm, focusing on the general pattern of stress behavior across the structure. The maximum principal stress plot (Figure 6a) shows that the majority of the glass panels experience low to moderate tensile stresses, with most of the structure remaining within safe tension limits for float glass. While localized stress intensification may occur around geometric transitions, no widespread or concentrated high-tensile zones are observed in the smoothed stress contours, suggesting a well-distributed tensile load path aligned with the shell action of the bridge. The minimum principal stress distribution (Figure 6b), corresponding to compressive stress, reveals a more uniform compressive field, with stress magnitudes increasing near support regions and joint intersections. This pattern is characteristic of a form-active shell structure and reflects efficient in-plane compressive force transfer. Although peak values may occur in isolated regions, the compressive behavior remains within the material's safe limits and contributes to the overall stability of the system.

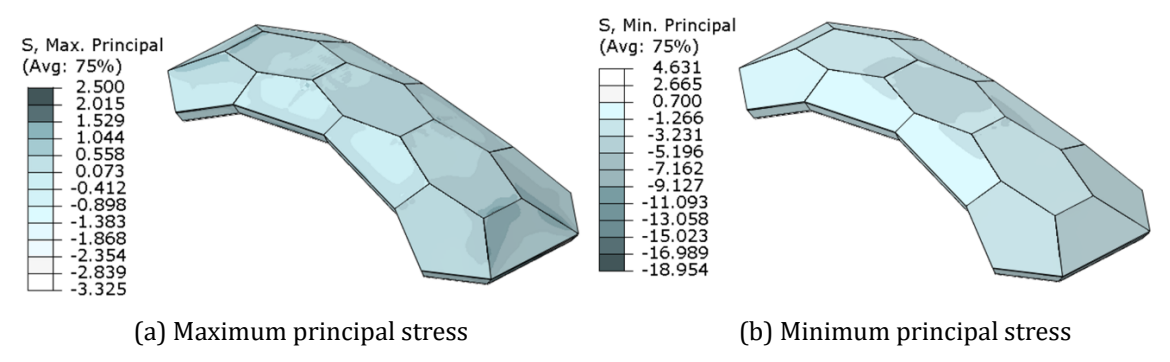


Figure 6. Stress distribution in 3.3-m glass bridge prototype

4. Results of 10-m bridge

Figure 7 illustrates the distribution of principal stresses in the 10-meter modular glass bridge, derived from the finite element simulation under a displacement of 10 mm. These stress contours reveal the overall mechanical behavior of the shell structure, emphasizing the influence of span length, segmental interactions, and geometric curvature on stress distribution. The maximum principal stress plot (Figure 7a) shows a broader spread of tensile stress across multiple Hollow Glass Units (HGUs), particularly along the longitudinal interfaces and midspan zones. Compared to the 3.3-meter prototype, where tensile demands were localized, the longer span results in more widespread tension-prone areas. This reflects the increased structural sensitivity to geometric imperfections and joint flexibility in larger-scale assemblies. The minimum principal stress plot (Figure 7b) shows a correspondingly broader distribution of compressive stress, concentrated near the central span and interface connections. The pattern aligns with expected load paths in a shell-dominant system, indicating that the bridge is effectively transmitting loads through in-plane compression. Overall, the stress patterns suggest that while the structure benefits from shell-like behavior, increased tensile activity in the upper deck requires careful attention in design, particularly in joint detailing and material selection, to mitigate fracture risks and ensure durability under service conditions.

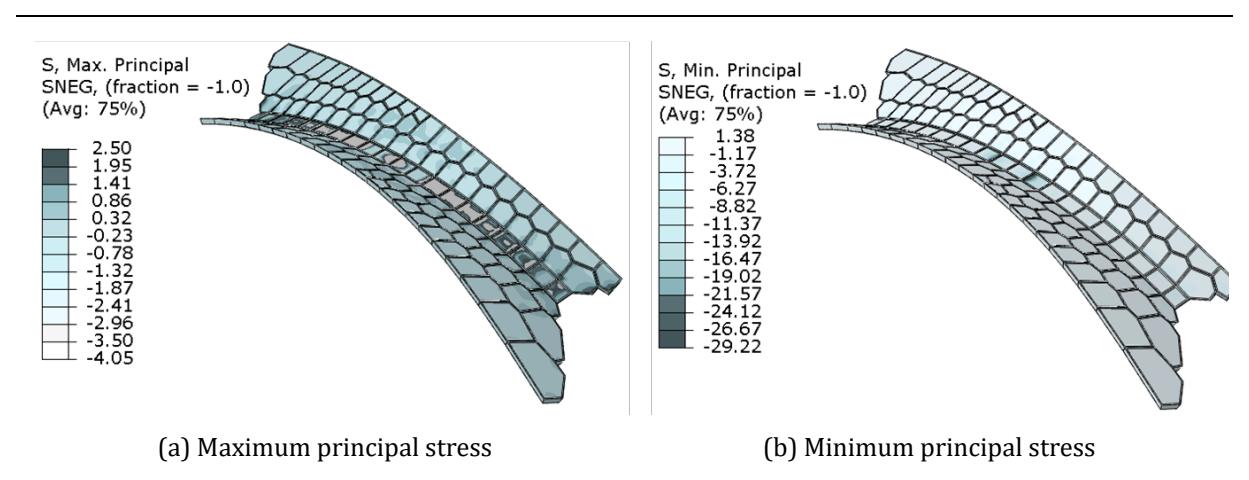


Figure 7. Stress distribution in 10-m glass bridge prototype

5. Conclusion

This study presented a validated finite element modeling approach for analyzing the structural performance of a modular pedestrian glass bridge composed entirely of interlocking Hollow Glass Units (HGUs). The model was calibrated against experimental data from a full-scale 3.3-meter prototype, capturing key behaviors such as stress distribution, inter-segment deformation, and post-loading recovery. A simplified micro-modeling strategy was employed to maintain a balance between computational efficiency and mechanical accuracy, incorporating essential features like tie constraints, frictional and cohesive contacts, and accurate material definitions for glass and acrylic. The validated model was then extended to simulate a 10-meter bridge, which introduced over 280 contact interactions. A hybrid contact strategy, comprising both frictional and cohesive elements, was critical for ensuring geometric stability and realistic load transfer across segments. Principal stress analysis confirmed that the structure remains predominantly compression-controlled, consistent with the design intent derived from Polyhedral Graphic Statics (PGS). Local tensile zones identified in the glass were generally within the acceptable stress limits for float glass throughout most of the structure; however, elevated stress concentrations were observed in certain regions, warranting closer attention in design and detailing. The outcomes demonstrate that with calibrated contact properties and careful abstraction of interfacial components, large-scale modular glass structures can be accurately modeled using a reduced yet representative FEM framework. This methodology supports future applications of transparent, compression-based structural systems and offers a scalable pathway for the design and analysis of glass bridges beyond the prototype scale.

Acknowledgements

This research was partially supported by the National Science Foundation Future Eco Manufacturing Research Grants NSF, FMRG-2037097 CMMI and NSF CAREER-1944691 CMMI.

References

[1] S. Hussain, P. S. Chen, D. Hassanlou, M. Bolhassani and C. Bedon. "Bending and lateral-torsional buckling investigation on glass beams for frameless domes," *Results in Engineering*, 21, p. 101962, 2024.

Proceedings of the IASS Annual Symposium 2025 The living past as a source of innovation

- [2] Y. Lu, A. Seyedahmadian, P. A. Chhadeh, M. Cregan, M. Bolhassani, J. Schneider...& M. Akbarzadeh. "Funicular glass bridge prototype: design optimization, fabrication, and assembly challenges," *Glass Structures & Engineering*, vol. 7, no. 2, pp. 319-330, 2022.
- [3] G. A. Gogotsi, and S. P. Mudrik. "Glasses: new approach to fracture behavior analysis," *Journal of non-crystalline solids*, vol. *356*, no.20-22, pp. 1021-1026, 2010.
- [4] B. Jiang, M. Atif, Y. Ding, Y. Guo, and & Y. Li. "An experimental study on the dynamic flexural tensile behavior of glass," *Engineering Fracture Mechanics*, 266, p. 108417, 2022.
- [5] M. Akbarzadeh, T. Van Mele, and P. Block. "Three-dimensional graphic statics: Initial explorations with polyhedral form and force diagrams," *International Journal of Space Structures*, vol. 31 no. 2-4, pp. 217-226, 2016.
- [6] M. Akbarzadeh, A. Nejur, and P. A. Chhadeh. "Polyhedral graphic statics for spatial compression-only structures," *Computer-Aided Design*, 134, p. 103003, 2021.
- [7] M. Bolhassani, M. Akbarzadeh, M. Mahnia, and R. Taherian. "On structural behavior of a funicular concrete polyhedral frame designed by 3D graphic statics," In *Structures* vol. 14, pp. 56-68, 2018.
- [8] J. R. Yost, J. H. Chacon, Y. Lu, M. Akbarzadeh, D. Bolhassani, F. Yavartanoo, ... and J. Schneider. "Experimental behavior of a prototype 3m-span modular glass pedestrian bridge," In *Challenging Glass Conference Proceedings* vol. *9*, 2024.
- [9] D. Bolhassani, D. Hassanlou, F. Yavartanoo, M. Akbarzadeh, Y. Lu, J. R. Yost, J. H. Chacon, J. Schneider, P. A.Chhadeh. "Numerical analysis with experimental verification of a multi-layer sheet-based funicular glass bridge," In *Challenging Glass Conference Proceedings*, 2024.
- [10] M. Bolhassani, A. A. Hamid, A. C. Lau, & F. Moon. "Simplified micro modeling of partially grouted masonry assemblages," *Construction and Building Materials*, 83, 159-173, 2015.